Adiabatic Coupling in the Helium and the Beryllium Series

Andreas Savin,[1] François Colonna,[1] and Jean-Marie Teuler[2]

[1]Laboratoire de Chimie Théorique (CNRS)
Université Pierre et Marie Curie
4, Place Jussieu
Case 137
F-75252 Paris, France

[2] CNRS-IDRIS
Batiment 506, B.P. 167
91403 Orsay Cedex, France

Version: May 20, 1997

Introduction

Switching on the electron-electron interaction has provided a means for a deeper understanding of the Kohn-Sham formalism [1, 2, 3, 4]. In recent years this adiabatic coupling was also used to produce density functionals (see *e.g.*, Ref. [5]) among which the so-called hybrid schemes [6] had a great success. It was conjectured that the local density approximation works well for values of the coupling constant close to one (cf. [7]). Little is known, however, about the actual behavior of the correlation energy in real systems (see, *e.g.*, [8]). The present paper shows results for simple systems (the helium and the beryllium series) often used as a benchmark in density functional calculations, as they are known not to behave properly in the local density approximation (LDA) [9].

In the following some adiabatic connection formulas will be re-derived, then some calculations will be presented along with a comparison with LDA [10] and the Perdew-Burke-Ernzerhof (PBE) generalized gradient approximation [11].

Some adiabatic connection formulas

The adiabatic connection provides a direct link between calculations using effective one-particle Hamiltonians and those using the exact one. In density functional theory (DFT) it is natural to use the Kohn-Sham Hamiltonian as the first one. Thus Harris and Jones proposed [2]:

$$\hat{H}^{\lambda} = \hat{H}^{0} + \lambda(\hat{V}_{ee} + \hat{V}_{ext} - \hat{V}_{KS}) \tag{1}$$

where

$$\hat{H}^{0} = \hat{H}^{\lambda=0} = \hat{H}_{KS} = \hat{T} + \hat{V}_{KS} \tag{2}$$

$\hat{T}, \hat{V}_{ee}, \hat{V}_{ext}, \hat{V}_{KS}$ are the operators for the kinetic energy, for the interaction between the electrons, between the electrons and the external (*e.g.*, nuclear) field, and the Kohn-Sham potential, respectively. λ is the coupling constant, which will be considered to vary between zero and one in this paper. For $\lambda = 0$ (viz., $\lambda = 1$) the Kohn-Sham (viz., the exact) Hamiltonian is obtained.

One of the advantages using the Kohn-Sham Hamiltonian is that it yields the exact density. It is possible to keep this property for all λ by a slight change in the definition of $\hat{H}^{\lambda}$ [3, 4]. * In this paper, we will pursue, however, the adiabatic connection as proposed by Harris and Jones (Eq. 1). We have the following arguments for doing it:

- The relative simplicity of obtaining $\langle \hat{H}^{\lambda} \rangle$ not keeping the density fixed, with a standard configuration interaction (CI) program. (In our case we used Molpro [13]).
- It gives the same value for the correlation energy (as defined in DFT).
- The change in the density can be calculated. A program trying to keep the density constant would have a criterion of analyzing the difference between the density at $\lambda \neq 1$ and at $\lambda = 1$. Such a criterion has been checked, and shown to be satisfied within an accuracy comparable to the error produced by using a finite number of Slater determinants and Gaussian basis functions in the CI calculation. This might not be very surprising, as the density at $\lambda = 0$ and $\lambda = 1$ are required to be the same.

*The Hohenberg-Kohn theorem [12] can be applied to any λ. The correct density is imposed by adding a potential V^{λ}

Let us first define some quantities. The energy, at coupling strength λ is:

$$E^{\lambda} = \langle \Psi^{\lambda} \mid \hat{H}^{\lambda} \mid \Psi^{\lambda} \rangle \tag{3}$$

where Ψ^{λ} is the antisymmetric minimizing wavefunction. $\Psi^{\lambda=0}$ is – in the absence of degeneracy – a Slater determinant (the Kohn-Sham determinant). The correlation energy (in density functional context) at coupling strength λ is:

$$\tilde{E}_c^{\lambda} = \langle \Psi^{\lambda} \mid \hat{H}^{\lambda} \mid \Psi^{\lambda} \rangle - \langle \Psi^{\lambda=0} \mid \hat{H}^{\lambda} \mid \Psi^{\lambda=0} \rangle \tag{4}$$

For $\lambda = 1$, $\tilde{E}_c^{\lambda}$ becomes the usual (density functional) correlation energy, while $\tilde{E}_c^{\lambda=0} = 0$. Keeping the density ($n$) constant for all λ one gets similarly:

$$E_c^{\lambda}[n] = \langle \Psi_n^{\lambda} \mid \hat{T} + \lambda \hat{V}_{ee} \mid \Psi_n^{\lambda} \rangle - \langle \Psi_n^{\lambda=0} \mid \hat{T} + \lambda \hat{V}_{ee} \mid \Psi_n^{\lambda=0} \rangle \tag{5}$$

where Ψ_n^{λ} is the minimizing antisymmetric wavefunction with the supplementary constraint that it yields n (see, *e.g.*, [14]). † Eq. 5 shows that $E_c^{\lambda}[n]$ is a universal density functional (viz., it depends on n alone).

As Ψ_n^{λ} has to satisfy a supplementary constraint with respect to Ψ^{λ} we have:

$$\tilde{E}_c^{\lambda} \leq E_c^{\lambda}[n] \tag{6}$$

Let us now show some properties of $\tilde{E}_c^{\lambda}$. Following Harris and Jones in using the Hellmann-Feynman theorem:

$$\begin{aligned}
\frac{\partial \tilde{E}_c^{\lambda}}{\partial \lambda} &= \langle \Psi^{\lambda} \mid \frac{\partial \hat{H}^{\lambda}}{\partial \lambda} \mid \Psi^{\lambda} \rangle - \langle \Psi^{\lambda=0} \mid \frac{\partial \hat{H}^{\lambda}}{\partial \lambda} \mid \Psi^{\lambda=0} \rangle \\
&= \langle \Psi^{\lambda} \mid \hat{V}_{ee} \mid \Psi^{\lambda} \rangle - \langle \Psi^{\lambda=0} \mid \hat{V}_{ee} \mid \Psi^{\lambda=0} \rangle + \\
&\quad \langle \Psi^{\lambda} \mid V_{ext} - \hat{V}_{KS} \mid \Psi^{\lambda} \rangle - \langle \Psi^{\lambda=0} \mid V_{ext} - \hat{V}_{KS} \mid \Psi^{\lambda=0} \rangle \\
&= \langle \Psi^{\lambda} \mid \hat{V}_{ee} \mid \Psi^{\lambda} \rangle - \langle \Psi^{\lambda=0} \mid \hat{V}_{ee} \mid \Psi^{\lambda=0} \rangle + \\
&\quad \int (n^{\lambda} - n)(v_{ext} - v_{KS})
\end{aligned} \tag{7}$$

n^{λ} is the density obtained from Ψ^{λ}; the last term on the r.h.s. disappears when $n^{\lambda} = n$. For obtaining numerical values of $\partial \tilde{E}_c^{\lambda} / \partial \lambda$ we have used the equivalent form:

$$\frac{\partial \tilde{E}_c^{\lambda}}{\partial \lambda} = \frac{\partial E_{\lambda}}{\partial \lambda} - \lim_{\lambda \to 0} \frac{\partial E_{\lambda}}{\partial \lambda} \tag{8}$$

Following Levy and Perdew (Eq. 65) of Ref. [15], one can obtain from the variation principle that:

$$\frac{\partial \tilde{E}_c^{\lambda}}{\partial \lambda} \leq 0 \tag{9}$$

While the two-body density matrix is needed in order to provide $\partial \tilde{E}_c^{\lambda} / \partial \lambda$ it can be readily shown that only the first-order density matrix is needed for $\partial (\tilde{E}_c^{\lambda} / \lambda) / \partial \lambda$ [16]. By applying again the Hellmann-Feynman theorem one gets:

$$\frac{\partial (\tilde{E}_c^{\lambda} / \lambda)}{\partial \lambda} = -\frac{1}{\lambda^2} [\langle \Psi^{\lambda} \mid \hat{T} + \hat{V}_{KS} \mid \Psi^{\lambda} \rangle - \langle \Psi^{\lambda=0} \mid \hat{T} + \hat{V}_{KS} \mid \Psi^{\lambda=0} \rangle] \tag{10}$$

† The contribution of the external potential are the same in $\langle \hat{H}^{\lambda} \rangle$ for all λ and disappear on the r.h.s of Eq. 5.

It follows from the preceding equation, and from the fact that $\Psi^{\lambda=0}$ is minimizing $\hat{T}$, that:

$$\frac{\partial \tilde{E}_c^\lambda/\lambda}{\partial \lambda} \leq 0 \tag{11}$$

From Eqs. 7,10 one gets:

$$\begin{aligned}\tilde{E}_c^\lambda &= \int_0^\lambda d\lambda[\langle \Psi^\lambda \mid \hat{T} + \hat{V}_{KS} \mid \Psi^\lambda\rangle - \langle \Psi^{\lambda=0} \mid \hat{T} + \hat{V}_{KS} \mid \Psi^{\lambda=0}\rangle] + \\ &\int_0^\lambda d\lambda \int (n^\lambda - n)(v_{ext} - v_{KS}) \\ &= -\lambda \int_0^\lambda \frac{d\lambda}{\lambda^2}[\langle \Psi^\lambda \mid \hat{T} + \hat{V}_{KS} \mid \Psi^\lambda\rangle - \langle \Psi^{\lambda=0} \mid \hat{T} + \hat{V}_{KS} \mid \Psi^{\lambda=0}\rangle]\end{aligned} \tag{12}$$

$\tilde{E}_c^\lambda$ in the He- and the Be-series

Reliable densities of iso-electronic ions were obtained from configuration interaction calculations [13]. Uncontracted even tempered basis sets were used (see Appendix). One-electron systems were treated at Hartree-Fock level. Two- and three-electron systems were described within CI with single and double excitations; in the Be-series, the orbitals were determined in a multi-configuration calculation using the determinants in the space including the 2s and 2p orbitals, from which singly and doubly excited determinants were produced. The (quantum chemical) correlation energies obtained are shown in Table 1, where they are compared to estimates of the 'exact' correlation energies.

Next, Kohn-Sham potentials were generated from these densities. For the He series, only the direct inversion of the Kohn-Sham equation was needed:

$$v_{KS} = \epsilon - \frac{1}{2}\frac{\nabla^2\varphi}{\varphi} \tag{13}$$

where $\varphi = \sqrt{n/2}$ and ϵ equals minus the ionization potential of the two-electron series. In the Be-series the algorithm is described in Refs. [17, 18], some details are given in the Appendix.

Finally, the matrix elements of the one-body matrix were modified in the program, according to Eq. 1, and the two-electron integrals were multiplied by λ. CI calculations were performed for ~ 30 values of λ between 0 and 1. In order to measure the change of the density we have also calculated the integral:

$$\int \frac{(n^\lambda(\mathbf{r}_1) - n(\mathbf{r}_1))(n^\lambda(\mathbf{r}_2) - n(\mathbf{r}_2))}{r_{12}} d^3r_1 d^3r_2 \tag{14}$$

(cf. Eq. 43 of Ref. [18] and Eq. 7). The maximum absolute value we get for this integral is around $\lambda \approx 0.4$ and is of the order of 10^{-5} hartree, indicating that no important change of the density is present when $0 < \lambda < 1$.

The values of $\tilde{E}_c^\lambda$ are plotted in Fig. 1a. Fig 1b shows the ratio $\tilde{E}_c^\lambda/E_c$. All curves become similar. This support that an universal behavior of $\tilde{E}_c^\lambda/E_c \approx f(\lambda)$ might be used in some computational scheme for approximating E_c, if, at a given value $\lambda^\star$ of λ, $E_c^{\lambda^\star}$ can be estimated.

$$E_c = E_c^{\lambda^\star}/f(\lambda)$$

An error in $f(\lambda)$, δf propagates however as $\delta\tilde{E}_c^\lambda = -\tilde{E}_c^{\lambda^\star}\delta f/f^2$ and $f \leq 1$.

Instead of tabulating the values for $\tilde{E}_c^\lambda$, an approximate fit was made with *Mathematica* [19]:

Table 1. Correlation energies in mhartree. The 'exact' values according to the traditional definition of Wigner and Löwdin [23, 24] are taken from Ref. [25], and correspond to the difference between corrected experimental values and Hartree-Fock energies. The 'CI-HF'-values correspond to the difference between our (limited basis set) configuration interaction and Hartree-Fock calculations. The 'DF'-values are those which were obtained with the same basis sets, but according to the definitions given in Eqs. 4 or 10.

Atom	exact	CI-HF	DF
H^-	-42.0	-39.7	-41.9
He	-42.0	-41.6	-41.6
Li^+	-43.5	-42.9	-42.9
Be^{2+}	-44.3	-43.6	-43.6
B^{3+}	-44.7	-44.0	-44.0
C^{4+}	-45.1	-44.3	-44.3
N^{5+}	-45.3	-44.5	-44.5
O^{6+}	-45.5	-44.6	-44.9
F^{7+}	-45.6	-44.8	-45.0
Ne^{8+}	-45.7	-44.9	-45.1
Li^-	-72.7	-69.0	-75.8
Be	-94.3	-90.9	-92.8
B^+	-111.4	-108.8	-111.5
C^{2+}	-126.4	-123.8	-127.8
N^{3+}	-140.5	-137.8	-143.4
O^{4+}	-154.1	-151.2	-158.7
F^{5+}	-167.3	-163.9	-173.9
Ne^{6+}	-180.4	-176.8	-189.9

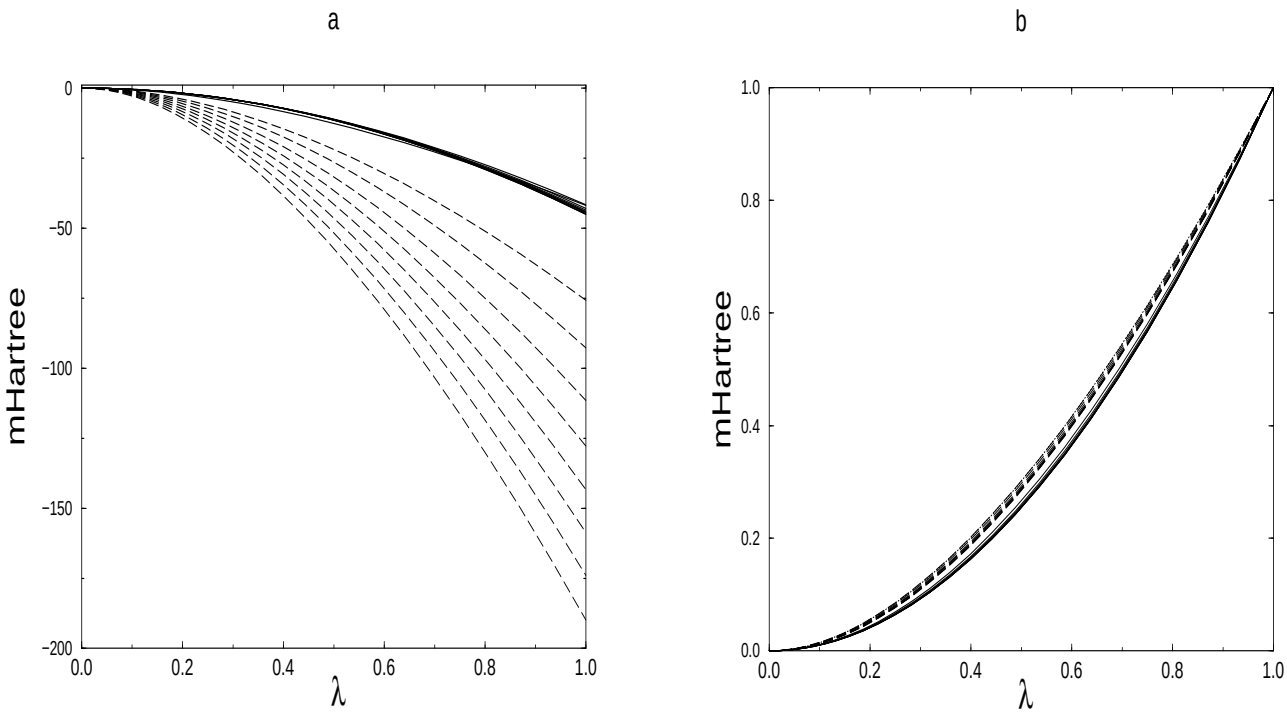

Figure 1. a) Correlation energies $\tilde{E}_c^\lambda$ in the He- and in the Be-series calculated from Eq. 4. All the curves in the He-series (solid lines) appear superimposed at this resolution ; the curves of Li^- to Ne^{6+} (dashed lines) can be easily identified by the monotonic decrease of $\tilde{E}_c^\lambda$ with Z within the series. b) Ratio $\tilde{E}_c^\lambda/E_c$. The H^- curve appears on top of the dashed Be-series curve.

$$\tilde{E}_c^\lambda = E_c \sum_{i=2}^{i_{max}} e_i \lambda^i \tag{15}$$

The values of the coefficients e_i are given in Table 2 (E_c are given in column 'DF' of Table 1).

As this is not an expansion in terms of λ, the coefficients e_i are those of a perturbational series. They also will change with the degree of the polynomial (i_{max}) used for fitting. We have noticed, however, that the coefficients of the lower powers do not change significantly with the increase of i_{max}.

Note that the confluence of curves at $\lambda \to 0$ in Fig. 1b comes from the $\approx \lambda^2$ behavior of $\tilde{E}_c^\lambda/\tilde{E}_c$. The e_2 coefficient, is however, system sensitive. For the two-electron systems (with Z $\geq$ 2) it is close to 1. Near-degeneracy increases their values. For a uniform electron gas e_2 has a $\ln\lambda$ divergence.

Fig. 2 and 3 show $\partial\tilde{E}_c^\lambda/\partial\lambda$ and $\partial(\tilde{E}_c^\lambda/\lambda)/\partial\lambda$ vs. λ respectively. Note that, in accordance with Eq. 9 $\partial\tilde{E}_c^\lambda/\partial\lambda$ is monotonically decreasing, and, that $\partial(\tilde{E}_c^\lambda/\lambda)/\partial\lambda$ is always negative according to Eq. 11.

Note also that, in accordance to Levy's conjecture [20] the curvature of $\partial\tilde{E}_c^\lambda/\partial\lambda$ is positive and also that all $\partial(\tilde{E}_c^\lambda/\lambda)/\partial\lambda$ increase monotonically with λ.

Comparison with LDA and GGA approximations

Let us now compare our results with approximate ones (LDA or PBE) which were generated via the scaling relationship [21, 22]:

$$E_c^\lambda[n] = \frac{1}{\lambda^2} E_c[n_{1/\lambda}] \tag{16}$$

Table 2. Coefficients of λ^i of the polynomial fit to $\tilde{E}_c^\lambda/E_c$, cf. Eq. 15 (in mhartree).

Atom	e_2	e_3	e_4	e_5
H^-	1.5496	-0.8892	0.4673	-0.1277
He	1.1428	-0.1640	0.0237	-0.0025
Li^+	1.0873	-0.0951	0.0084	-0.0006
Be^{2+}	1.0633	-0.0681	0.0055	-0.0007
B^{3+}	1.0494	-0.0521	0.0029	-0.0002
C^{4+}	1.0407	-0.0426	0.0022	-0.0003
N^{5+}	1.0343	-0.0354	0.0010	0.0000
O^{6+}	1.0300	-0.0314	0.0017	-0.0003
F^{7+}	1.0266	-0.0278	0.0016	-0.0004
Ne^{8+}	1.0234	-0.0234	-0.0003	0.0003
Li^-	1.4412	-0.7618	0.4392	-0.1186
Be	1.3507	-0.5019	0.1863	-0.0351
B^+	1.3332	-0.4580	0.1495	-0.0246
C^{2+}	1.3594	-0.5091	0.1836	-0.0340
N^{3+}	1.3918	-0.5736	0.2282	-0.0464
O^{4+}	1.4405	-0.6759	0.3038	-0.0684
F^{5+}	1.5108	-0.8304	0.4246	-0.1050
Ne^{6+}	1.5858	-1.0058	0.5717	-0.1518

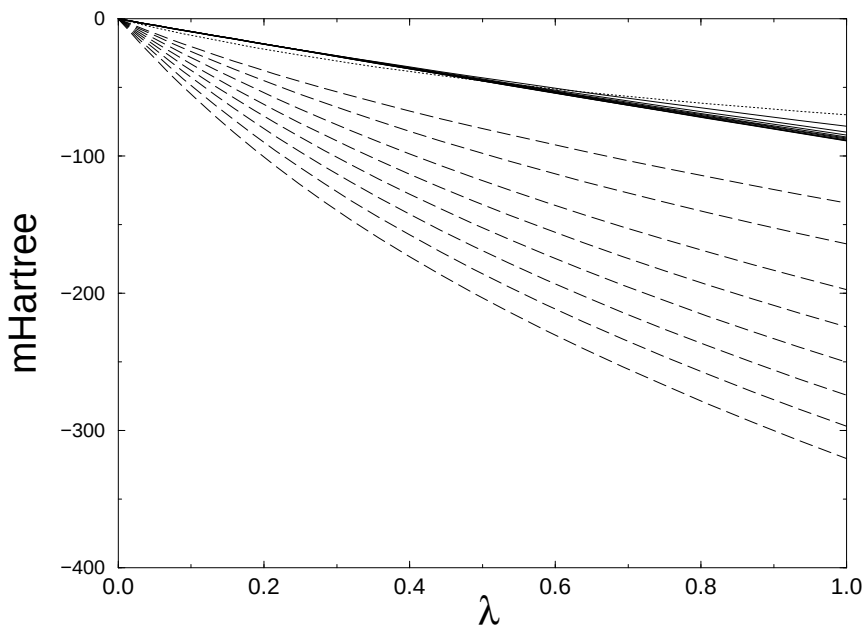

Figure 2. Curves of $\partial\tilde{E}_c^\lambda/\partial\lambda$ calculated from Eq. 8 for the He-series (solid lines, except H^- : dotted line) and for the Be-series (dashed lines); $\partial\tilde{E}_c^\lambda/\partial\lambda$ decreases with Z.

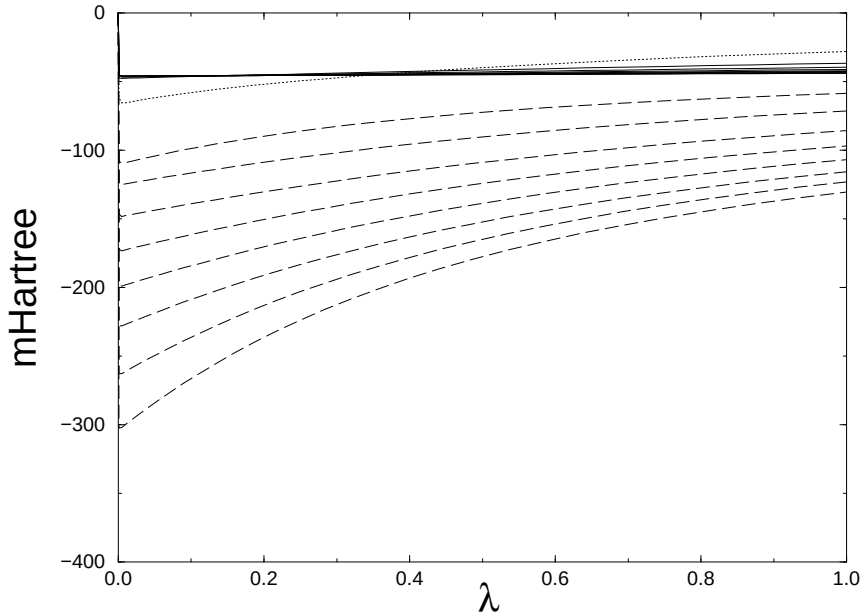

Figure 3. Curves of $\partial(\tilde{E}_c^\lambda/\lambda)/\partial\lambda$ calculated from Eq. 10 for the He-series (solid lines, except H^- : transversal dotted line) and for the Be-series (dashed lines); $\partial(\tilde{E}_c^\lambda/\lambda)/\partial\lambda$ decreases with Z.

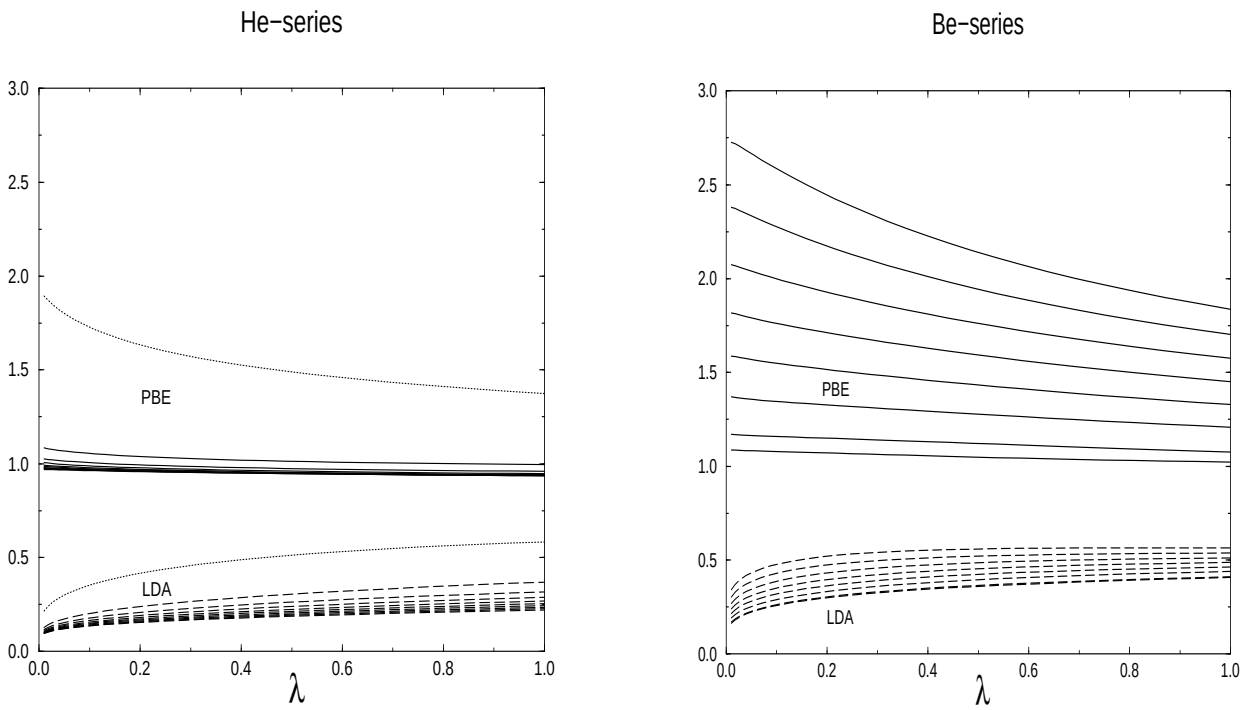

Figure 4. Ratio between exact values of $\tilde{E}_c^\lambda$ calculated from Eq. 4 and those calculated from LDA (dashed lines) or from PBE (solid lines), as a function of λ. All curves appear in the order of their atomic number. Left side: He-series (the two dotted line curves correspond to H^-). Right side: Be-series

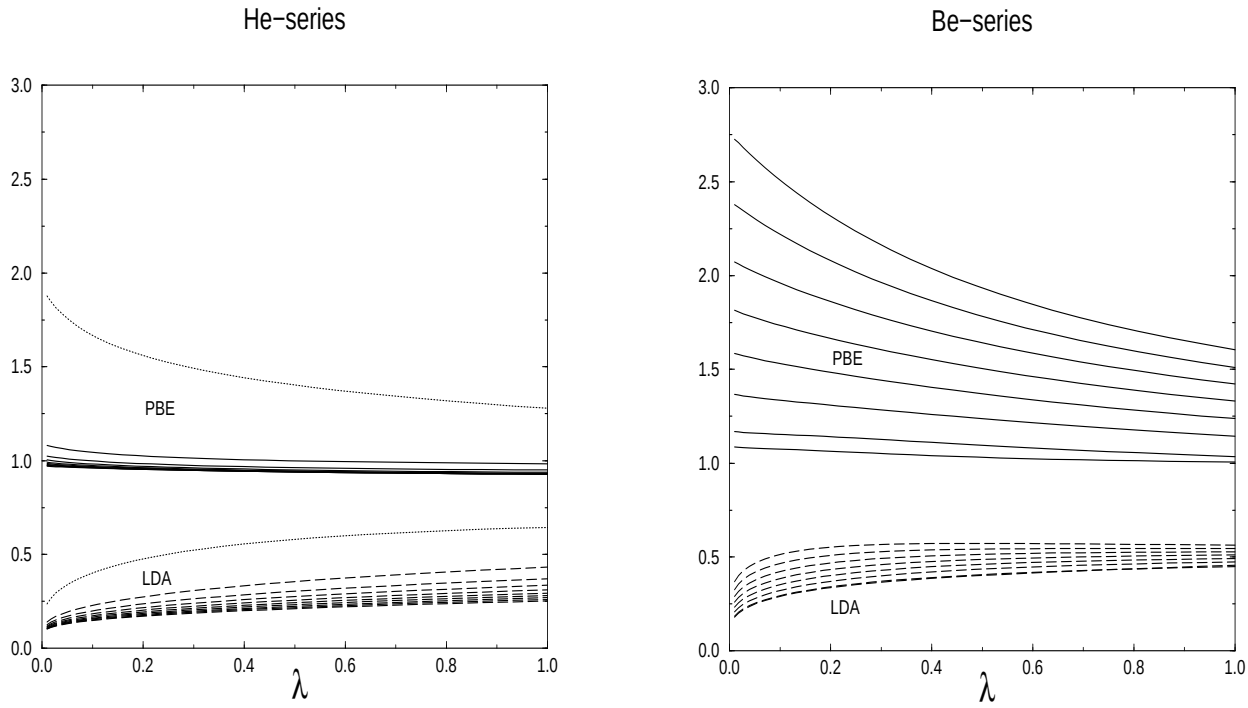

Figure 5. Ratio between exact values of $\partial\tilde{E}_c^\lambda/\partial\lambda$ calculated from Eq. 8 and those calculated from LDA (dashed lines) or from PBE (solid lines), as a function of λ. All curves appear in the order of their atomic number. Left side: He-series (the two dotted line curves correspond to H^-). Right side: Be-series

where n_α is the scaled density $n_\alpha(r) = \alpha^3 n(\alpha r)$. We show in Fig. 4 the ratio between $\tilde{E}_c^\lambda$ and the values obtained in density functional approximation. Please note the quite good agreement between the exact and PBE values for He and the positive ions of its series. In the Be-series the worsening of the agreement at small λ and large Z is conspicuous. Note also the similarity of the behavior of H^- and the ions of the Be-series. We believe that this is due to the important role of the 2s orbitals in describing the correlation in H^-.

Let us now analyze the quality of the approximate derivative of $\tilde{E}_c^\lambda$. We show in Fig. 5 the ratio between $\partial\tilde{E}_c^\lambda/\partial\lambda$ obtained from our calculations and that obtained from the LDA and the PBE approximations, respectively. While with PBE the ratio stays close to 1 for He and the positive ions of the He-series and at the start of the Be-series, in all the other cases the discrepancy is significant.

It was conjectured that LDA is a better approximation for $\partial\tilde{E}_c^\lambda/\partial\lambda$ when $\lambda \to 1$ [7]. We show in Fig. 6a the ratio between $\partial\tilde{E}_c^\lambda/\partial\lambda$ and the LDA or PBE approximations to it at $\lambda = 1$. Please note the similarity of the ratio with that of the exact/approximate correlation energies (Fig. 6b).

Again, a significant improvement of PBE over LDA is manifest in the He-series. In the Be-series a linear increase of the error is, however, also present in PBE.

The simplest approximation for E_c based on the adiabatic scaling is to make a linear approximation for $\partial\tilde{E}_c^\lambda/\partial\lambda$ (cf. Ref.[7] and references therein). This would yield

$$E_c \approx 1/2\left(\partial\tilde{E}_c^\lambda/\partial\lambda\right)_{\lambda=1} \tag{17}$$

(remember that $\left(\partial\tilde{E}_c^\lambda/\partial\lambda\right)_{\lambda=0} = 0$).

In order to show the deviation from this simple approximation we give in Table 3 the ratio:

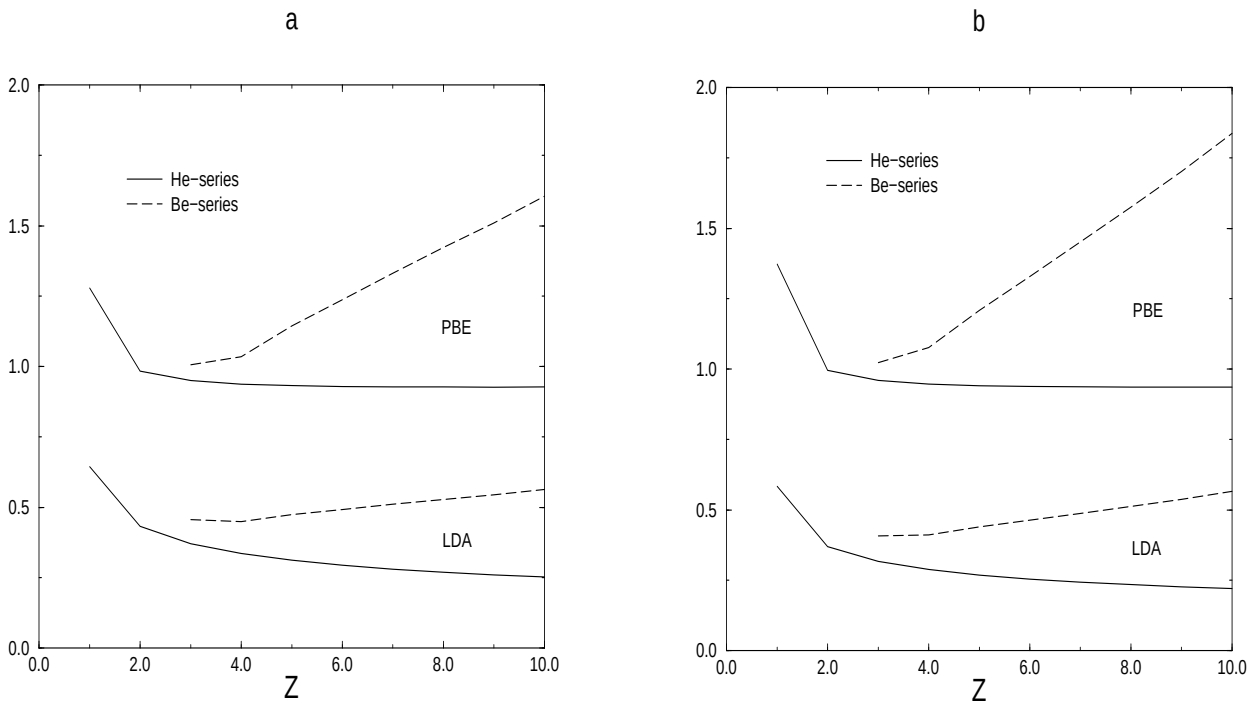

Figure 6. a) Ratio of correlation energies derivatives $\left(\partial \tilde{E}_c^{\lambda}/\partial\lambda\right)_{\lambda=1}$ calculated from Eq. 8. and those calculated from LDA (lower set of curves) or from PBE (upper set of curves), plotted against the nuclear charge Z. He-series are in solid lines and Be-series in dashed lines, b) the same for correlation energies E_c calculated from Eq. 4

Table 3. Deviation from the linear approximation to E_c (cf. Eq. 17,18)

Atom	d
He series	
H^-	0.166
He	0.062
Li^+	0.040
Be^{2+}	0.030
B^{3+}	0.023
C^{4+}	0.019
N^{5+}	0.017
O^{6+}	0.017
F^{7+}	0.015
Ne^{8+}	0.014
Be series	
Li^-	0.115
Be	0.116
B^+	0.116
C^{2+}	0.121
N^{3+}	0.128
O^{4+}	0.136
F^{5+}	0.147
Ne^{6+}	0.157

Table 4. Central exponent α_c of the (21s, 7p, 5d, 3f) and (21s, 9p, 5d, 3f) even tempered basis sets in the He and Be-series.

Atom	s	p,d,f
He series		
H^-	8	0.5
He	40	3
Li^+	86	8
Be^{2+}	350	15
B^{3+}	475	23
C^{4+}	663	34
N^{5+}	990	48
O^{6+}	1200	65
F^{7+}	1612	83
Ne^{8+}	2030	100
Be series		
Li^-	1.8	0.5
Be	4	1
B^+	4.6	3.3
C^{2+}	10	5
N^{3+}	7.5	8
O^{4+}	12	11
F^{5+}	100	13
Ne^{6+}	130	15

$$d = 1 - \frac{1/2\left(\partial \tilde{E}_c^{\lambda}/\partial\lambda\right)_{\lambda=1}}{E_c} \tag{18}$$

Note that the non-linear character (d $\geq$ 0.12) is more pronounced in the Be-series and for H^-, than for He and the positive ions of its series (d $\leq$ 0.06).

Conclusion

Reliable data have been produced to show the change of the correlation energy with the adiabatic coupling constant. They show the progress made by gradient corrections as well as the room left for further improvement. We hope that the data presented in the paper will be of use in improving the approximate density functionals.

Appendix

Basis Sets

Even tempered Gaussian basis sets were used in the calculations. For each angular quantum number, M exponents α_n were produced by the rule $\alpha_n = \alpha_c \delta^{(2n-M-1)/2}$, $n = 1, \ldots$,M. The central exponents α_c, can be found in Table 4, $\delta = 2.1$.

The Kohn-Sham potential and orbitals in the Be-series

For the Be-series we used a numerical procedure to obtain the Kohn-Sham potential and orbitals which is often described in literature [28, 29, 30, 31, 18, 17]. For a given density, n, the orbitals are given by:

$$\begin{aligned} \varphi_1(r) &= \sqrt{n(r)/2}\cos(\theta(r)) \\ \varphi_2(r) &= \sqrt{n(r)/2}\sin(\theta(r)) \end{aligned}$$

Table 5. The parameters $\epsilon = \epsilon_1 - \epsilon_2$ and $\theta(0)$ calculated from Eq. 19, and $\epsilon_2 = -\mathrm{IP}$

Atom	ϵ	$\theta(0)$	ϵ_2
Li^-	-2.273	0.141	-0.022
Be	-3.882	0.199	-0.342
B^+	-6.722	0.236	-0.924
C^{2+}	-10.366	0.259	-1.759
N^{3+}	-14.749	0.274	-2.845
O^{4+}	-19.938	0.284	-4.182
F^{5+}	-25.950	0.292	-5.770
Ne^{6+}	-32.739	0.299	-7.608

where $\theta(r)$ is the solution of a second order differential equation (cf. Ref. [17, 18]). Its expression in spherical coordinates is:

$$\frac{d^2\theta(r)}{dr^2} + \frac{d\theta(r)}{dr}\left(\frac{2}{r} - \frac{1}{n(r)}\frac{dn(r)}{dr}\right) = \epsilon \sin(2\theta(r)) \tag{19}$$

subjected to the boundary conditions $\theta(\infty) = -\pi/2$, $\theta'(0)$ and $\theta'(\infty) = 0$, the orthogonality of φ_1 and φ_2 being enforced by a Lagrangian multiplier $\epsilon = \epsilon_1 - \epsilon_2$ (see, *e.g.*, Eq. 16 in Ref. [17]), where ϵ_1 and ϵ_2 are the energies associated with $\varphi_1(r)$ and $\varphi_2(r)$, and $n(r)$ is the 'CI' density. In order to obtain $\theta(r)$ the following procedure was followed:

1. Choose a value for ϵ and $\theta(r = 0)$
2. Solve the differential equation for these values yielding a set of possible φ_i and Kohn-Sham potential, v. [‡] The latter is obtained by inverting the Kohn-Sham equation (cf. Eq. 18 of Ref. [17]) for the higher eigenvalue ϵ_2 (taken from the ionization energy IP as given by the configuration interaction calculation, see Table 5).
3. Calculate the energy of the non-interacting system for the potential just obtained (by using the Hartree-Fock program [13]): $E[v]$.
4. Calculate $E[v] - \int v(r)n(r)d^3r$

According to Ref. [27], Eq. 3.17 this will be maximal when v is the Kohn-Sham potential. We thus repeat the steps 1 to 4 with different values of ϵ and $\theta(0)$ in order to maximize the above expression (by using the simplex procedure [26]).

The resulting values of ϵ and $\theta(0)$ are given in Table 5.

Acknowledgements

We are grateful to H.-J. Werner for providing us the program Molpro and to J.P. Perdew for sending us the PBE subroutines. We would also like to thank O. Bokanowski, M. Levy and C. Umrigar for stimulating discussions.

[‡] We have used the routine `odeint` of Ref. [26], because of the stiffness of the differential equation (19), which proved to be difficult to solve with other procedures.

REFERENCES

1. W. Kohn and L. Sham, Phys. Rev. **A140**, 1133 (1965).
2. J. Harris and R.O. Jones, J. Phys. F, **4**, 1170 (1974).
3. D.C. Langreth and J.P. Perdew, Solid State Commun. **17**, 1425 (1975).
4. O.Gunnarsson and B.I. Lundqvist, Phys. Rev. B **13**, 4274 (1976).
5. Q. Zhao, M. Levy and R. G. Parr, Phys. Rev. **A 47**, 918 (1993).
6. A.D. Becke, J. Chem. Phys. **98**, 1372 and 5648 (1993)
7. K. Burke, J.P. Perdew, and M. Ernzerhof this volume.
8. R. Hood, M.Y. Chou, A.J. Williamson, G. Rajagopal, R.J. Needs, and W.M.C. Foulkes, Phys. Rev. Letters to appear.
9. J.P. Perdew, E.R. McMullen, and A. Zunger, 1981, Phys. Rev. A **23**, 2785.
10. S.H. Vosko, L. Wilk, H. Nusair, Can. J. Phys. **58**, 1200 (1980).
11. K. Burke, J.P. Perdew, and M. Ernzerhof, Phys. Rev. Letters, **77**, 3865 (1996).
12. P. Hohenberg and W. Kohn, Phys. Rev. **B136**, 864 (1964)
13. MOLPRO is a package of *ab initio* programs written by H.-J. Werner and P. J. Knowles, with contributions from J. Almlöf, R. D. Amos, M. J. O. Deegan, S. T. Elbert, C. Hampel, W. Meyer, K. Peterson, R. Pitzer, A. J. Stone, and P. R. Taylor.
14. M. Levy, Phys. Rev. A **43**, 4637 (1991).
15. M. Levy and J.P. Perdew, Phys. Rev., **A32**, 2010 (1995)
16. A. Savin, Phys. Rev., **A52**, R1805 (1995)
17. F. Aryasetiawan and M. J. Stott, Phys. Rev. **B 34**, 4401 (1986).
18. Q. Zhao and R. G. Parr, Phys. Rev. **A 46**, 2337 (1992).
19. Stephen Wolfram, The Mathematica Book, 3rd ed. Wolfram Media/Cambridge University Press, 1996.
20. M. Levy, in *Recent Developments and Applications of Modern Density Functional Theory*, edited by J. Seminario (Elsevier, Amsterdam, 1996)
21. M. Levy and J.P. Perdew, in *Sigle-Particle Density in Physics and Chemistry*, edited by N.H. March and B.M. Deb (Academic, London, 1987).
22. W. Yang, in *Density Matrices and Density Functionals*, edited by R. Erdahl and V.H. Smith, Jr (Reidel, Boston, 1987).
23. Wigner, Phys. Rev., **46**, 1002 (1934)
24. Lowdin, Phys. Rev., **97**, 1474 (1955)
25. S.J. Chakravorty, S.R. Gwaltney, E.R. Davidson, F.A. Parpia, and C. Froese Fischer, Phys. Rev., **A47**, 3649 (1993)
26. Numerical Recipes W.H. Press, S.A. Teukolsky, W.T. Vettrlimg, and B.P. Flannery, Cambridge Univ. Press (1992)
27. E.H.Lieb Int. J. Quant. Chem., 24, 243 (1983)
28. K.A. Dawson and N.H. March, J. Chem. Phys. **A 81**, 5850 (1984).
29. N.H. March and R.F. Nalewajski, Phys. Rev. **A 35**, 525 (1987).
30. A. Nagy and N.H. March, Phys. Rev. **A 39**, 5512 (1989).
31. A. Holas and N.H. March, Phys. Rev. **A 44**, 5521 (1991).
32. Q. Zhao and R. G. Parr, J. Chem. Phys. **98**, 543 (1993).